IEEE Access
Multidisciplinary | Rapid Review | Open Access Journal

Received October 26, 2017, accepted November 27, 2017, date of publication January 9, 2018,
date of current version February 28, 2018.

Digital Object Identifier 10.1109/ACCESS.2017.2789248

Broadband GaN Class-E Power Amplifier for Load Modulated Delta Sigma and 5G Transmitter Applications

TUSHAR SHARMA, (Student Member, IEEE), POUYA AFLAKI, (Member, IEEE), MOHAMED HELAOUI, (Member, IEEE), AND FADHEL M. GHANNOUCHI, (Fellow, IEEE)

Intelligent RF radio Laboratory, Department of Electrical and Computer Engineering, Schulich School of Engineering, University of Calgary, Calgary, T2N1N4, Canada

Corresponding author: Tushar Sharma (tsharm@ucalgary.ca)

This work was supported in part by the Natural Sciences and Engineering Research Council of Canada, in part by Alberta Innovates Technology Futures, and in part by the Canada Research Chairs Program.

ABSTRACT The paper presents a design of a broadband high-efficiency class-E power amplifier (PA) for the advanced efficiency enhancement architectures applications. A sequential load pull methodology to design broadband class-E power amplifiers using a packaged gallium nitride power transistor is presented. Two different broadband matching synthesis techniques have been proposed using lumped elements have been presented and implemented in the manuscript. A fourth-order low-pass impedance transformation topology is designed as the output matching network to provide the optimum load reflection coefficients in the targeted bandwidth (1.8–2.7 GHz). A combination of input and output matching network has been proposed in the manuscript to satisfy the given fractional bandwidth requirements. For practical validation, a Wolfspeed (Cree) CGH40025 package transistor has been used. Under continuous wave test condition the fabricated PA showed more than 50% power added efficiency (PAE) with up to 29 W output power for 40% fractional bandwidth from 1.8–2.7 GHz. Furthermore, the proposed broadband Class E PA is deployed in efficiency enhancement architecture like delta-sigma modulation based transmitters. The PA shows more than 48% PAE all over the frequency band when driven with a delta-sigma modulated LTE downlink signal while maintaining high signal quality and PA reliability.

INDEX TERMS broadband, class-E, delta-sigma, gallium nitride (GaN), lumped element, microstrip, switching-mode

I. INTRODUCTION

The future generation RF front-end systems demand highly efficient power amplifiers (PAs) which can handle multiple signal standards at different frequencies. All the signal coding, modulation, and conversion could be performed in digital processing frontend which is then amplified with a PA and sent to the antenna. This kind of transmitter is less complex in structure and can be switched easily between different signals and applications. Switching mode power amplifiers (SMPAs) have been a popular choice for realizing the high-efficiency operations. These SMPAs demands precise harmonic tuning and face narrow bandwidth constraint. The recent field of waveform engineering and harmonically manipulation has led to the extension of these inherent narrow band SMPAs to relatively broadband operation [1]–[13]. Despite being the promising candidates, these existing broadband amplifiers face limitations in terms of their deployment in wireless advanced efficiency enhancement architectures like Doherty, delta-sigma, envelope tracking etc. For practical implementation purposes, among the advanced transmitter architectures, delta-sigma modulation based transmitters are the most convenient ones to employ [14]–[20]. Since all the signal processing can be done in the FPGA and no additional hardware other than a single-ended SMPA is required. Moreover, in contrast to polar and LINC transmitters, in delta-sigma transmitters, the SMPA input signal is a bi-level pulse which is perfect to drive the PA as a switch.

Class-E power amplifier shows more promising performance to the input signal with different duty cycles, as it often occurs in delta-sigma modulation based transmitters,

compared to class-F and class-D SMPAs [4]. Moreover, a class-E PA is easier to design for broadband applications due to its output load impedance conditions, more precisely its high impedance load conditions for harmonic frequencies when compared with class-F and class-D SMPAs. In recent years some works have been done to design broadband class-E power amplifiers. The transistor is assumed to be an ideal switch with no output capacitance in [5] and a band-pass matching circuit is designed to provide the obtained optimum load under this ideal assumption, for the desired frequency band. In [8] more attention is paid to the input matching circuit such that the sine-wave input voltage is converted to a square-wave voltage at the gate of the transistor to enhance the switch-like operation. The broadband performance is simply achieved by an output series LC resonator. The output circuit in [10], consisting of a two-stage lumped element matching network followed by a band-pass Butterworth filter, transfers 50 Ω reference impedance to the theoretical optimum class-E load impedance at the fundamental frequency within the passband. Reactance compensation technique has been used in [11] to cancel out the output capacitance of the active device and achieve broadband performance in an MMIC design. A design methodology based on the nonlinear model of a transistor and by using low-pass matching structure is presented in [12] and [13].

All these broadband designs are either based on class-E theoretical optimum load impedance equation or commercial transistor models. Often times due to model inaccuracies, and non-linear charges the simulated and measured impedances exhibits a high impedance mismatch. As a result, the simulated and measured results show quite a lot discrepancies. Moreover, except [12] no clear systematic design approach is followed by these reported research works to synthesize both input and output matching circuits.

In this paper, a methodical design approach is presented to design a broadband class-E power amplifier which employs a packaged active device. Theoretical class-E optimum load equation is used to locate the required class-E load reflection coefficient region on the Smith chart and an optimum output matching circuit configuration is selected according to this study. On the other hand, the optimum input reflection coefficient is more dependent on the packaged device rather than the class of operation. For this reason, a predetermined circuit configuration cannot be proposed for input matching network. This circuit should be selected after obtaining optimum input reflection coefficients by source-pull measurements. This method can be applied to any device technology and operating frequency band.

This paper is organized as follows. In Section II, a generalized theory of class E operating principle amplifiers is presented. The matching network for broadband class E amplifiers is explained in Section III. A proof of concept and PA implementation is carried out in Section IV. The PA measurements are shown in section V of the paper.

II. CLASS-E OPERATION PRINCIPLE

In a Class-E PA, by taking advantage of the device output capacitance and selecting the fundamental load impedance, the drain current and voltage waveforms are engineered so that they do not overlap during the entire RF cycle. In addition, the drain voltage and its derivative should be set to zero when the transistor turns ON. This guarantees the zero voltage crossing at the instant of the transition from OFF to ON state resulting in no power dissipation. The transistor drain should be kept to open circuit at all harmonic frequencies. In a practical RF design, only the second and third harmonic impedances are considered since higher harmonic frequencies don't carry any considerable amount of power. The optimum fundamental load impedance for class-E operation is expressed in (1) [13].

$$Z_{Drain} = \begin{cases} Z_{opt,E} & f = f_0 \\ \infty & f = nf_0,\ n > 1 \end{cases}$$
$$Z_{opt,E} = \frac{0.58(1 + j1.14)}{5.42\omega C_{out}} \quad (1)$$

The optimum class-E load impedance is inversely proportional to both the device output capacitance and frequency of operation. Fig.1 shows the movement of the class-E ideal optimum load reflection coefficient in the Smith chart with a change in output capacitance and frequency of operation. By either increasing frequency or the device drain-source capacitance (C_{ds}) the optimum load moves towards the small impedance area in the Smith chart (short circuit in the extreme limit). High power devices generally have high periphery C_{ds} thereby increasing the matching complexities. The reference impedance (50 ohms) can be easily transferred to the optimum load with a simple matching network if the load is far from the small impedance area.

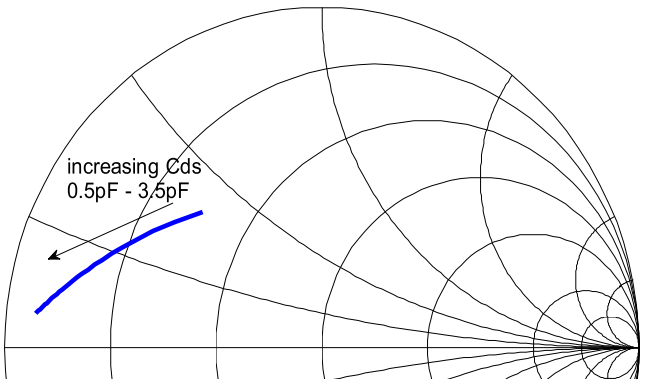

FIGURE 1. Class-E optimum load reflection coefficient for a fixed frequency/device output capacitance (2 GHz/2 pF) and variation of the device output capacitance/frequency (0.5 pF to 3.5 pF/0.5 GHz to 3.5 GHz).

There are 8 possible ways to create circuits with 2- element lumped component to transfer 50 ohms to an impedance in the Smith chart. In this paper, lumped element circuits are considered to attain a general method for designing class-E PAs. Alternatively, these circuits can be converted to distributed

circuits by replacing capacitances with low impedance open circuited stubs and inductances with high impedance short transmission lines according to (2) and (3) respectively.

$$\theta_C = \tan^{-1}(\omega \cdot C \cdot Z_0) \tag{2}$$

$$\theta_L = \frac{\omega \cdot L}{Z_0} \tag{3}$$

where θ_C and θ_L are electrical lengths of the equivalent transmission lines.

III. MATCHING NETWORK CONFIGURATIONS

In order to design a broadband class-E, PA input and output matching networks should be designed to provide optimum impedances for both input and output of the active device in the targeted pass-band. The first question to be answered is that what output matching topology should be used to transfer 50 Ω to the optimum load. In general, distributed and lumped elements are the two options to realize matching circuits. Transmission lines have a more sensitive response to the frequency variation than the lumped element components. This is actually considered as a drawback in a broadband design. On the other hand, lumped element components present a Self-Resonance Frequency (SRF) and Quality factor (Q) which should be carefully considered in the design process. Taking into account SRF of the commercially available capacitors, inductors and the Q of inductors, the design up to 4 GHz is realizable by lumped component structures which are preferred in distributed configurations for a wideband design. Therefore in this paper, the PA design is based on lumped component configurations. Inductors may be replaced by short narrow transmission lines to improve the performance of such components.

Since according to the theoretical class-E operation analysis the locus of the load reflection coefficient in the Smith chart is known, as illustrated in Fig. 1 then the load impedance matching circuit configurations are studied independently of the device and its measurement results. On basis of that, a possible candidate is predetermined in III (A). However, the input matching circuit configuration is strongly dependent on source-pull measurement results of the utilized transistor and should be selected after performing this type of measurement.

A. OUTPUT MATCHING NETWORK CONFIGURATIONS

As shown in Fig. 1 optimum load impedance for a class-E PA is complex with inductive nature that lies in the top left region of the Smith chart. In general, to transfer this reference impedance to the desired complex impedance in the Smith chart, there are 8 possible 2-element lumped circuits that can be used. Only 5 of them can map 50 ohms to an inductive complex impedance located in the top left region of the Smith chart. Fig. 2 depicts these five configurations.

Configurations d and f in Fig.2 have a high-pass response which is not appropriate for class-E output matching network since the circuit should provide open circuit (high impedance) at harmonic frequencies. Another two configurations, a and b,

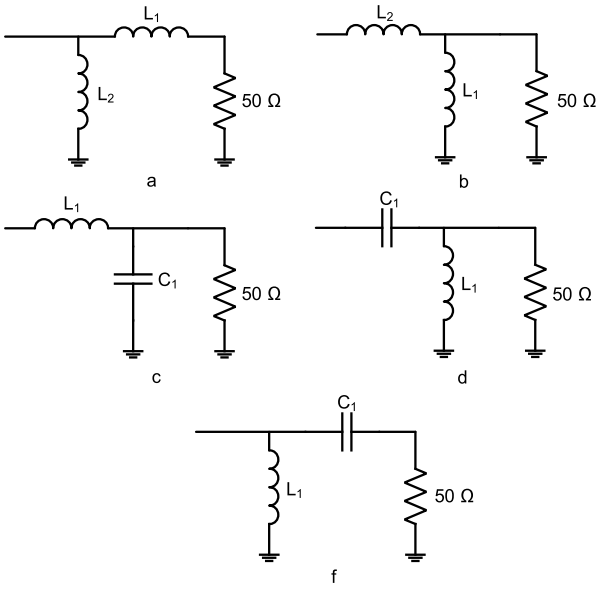

FIGURE 2. The 2-element lumped impedance transformation networks that can relocate 50 Ω to impedances in top left region of the Smith chart.

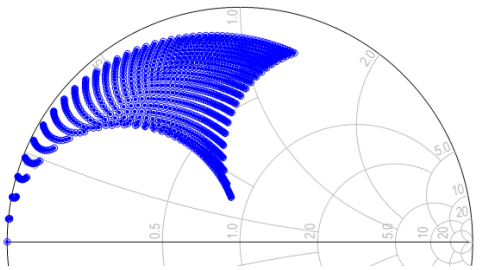

FIGURE 3. Simulated impedance design space for both L_1 and L_2 varying from 0 to 10 nH for topology (a).

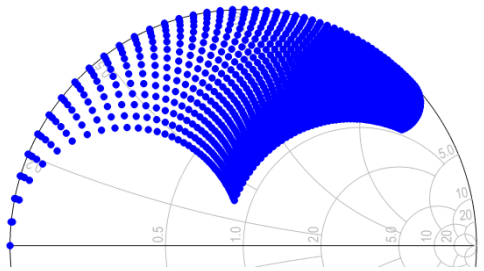

FIGURE 4. Simulated impedance design space for both L_1 and L_2 varying from 0 to 10 nH for topology (b).

have a band-pass response and can provide high impedance at the second and third harmonic respectively. However, they cover impedances in different areas of the top left region of the Smith chart. Fig. 3 and Fig. 4 shows design impedances of configurations a and b when L_1 and L_2 are varied from 0 to 10 nH at a frequency of 2 GHz. These two configurations may be a good choice for low frequency and low power designs where the optimum load reflection coefficient angle is close to 90° but they do not cover the design space

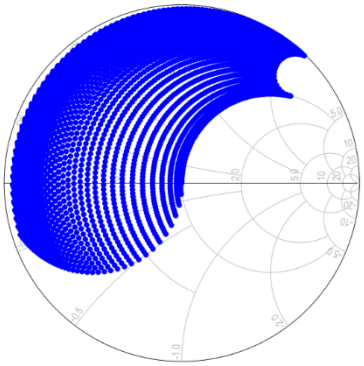

FIGURE 5. Simulated impedance design space for C_1 and L_1 varying from 0 to 10 pF and 0 to 10 nH respectively for topology (c).

targeted in this paper. To cater this problem, a configuration c with the low-pass response is considered to provide optimum class-E load impedance. This configuration provides a better high impedance for harmonic frequencies than configuration a and b respectively. Fig. 5 shows the covered impedance design area by configuration c when C_1 and L_1 are varied from 0-10 pF and 0-10 nH respectively. In addition, as can be seen by comparing Fig. 3 and Fig.4 with Fig.5 the configurations (a) and (b) are not able to provide complex impedances with small imaginary part while configuration c is perfectly capable of doing that. Small imaginary inductive impedance is exactly what should be presented at the output of an active device in an RF class-E high power amplifier. As mentioned earlier high-power devices (greater C_{ds}) require smaller complex optimum impedances than lower power devices. The approximate optimum output reflection coefficient area for higher and lower power designs are shown in Fig. 6 by considering the effect of device parasitics.

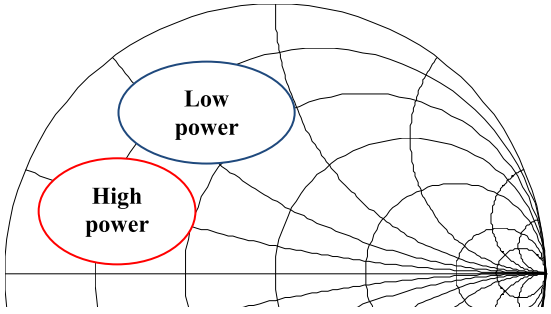

FIGURE 6. Optimum class-E load impedance areas for high power (greater C_{ds}) and lower power (smaller C_{ds}) devices.

Configuration c can fairly cover all the desired load reflection coefficient area for both low, high power class-E design space while configuration a and b would only cover the load impedance area for low power design with greater inductor values. Therefore, configuration c is picked to design the output matching circuit in this paper. To improve the bandwidth of these structures they can be used in ladder configuration by increasing the number of their stages. Although configuration c can also be employed in its band-pass configuration, this would increase the number of components which results in more complexity and higher loss. The design process of the output matching circuit is described in section IV (A).

B. INPUT MATCHING NETWORK

Input matching circuit in a class-E PA is designed so that maximum gain can be obtained. After designing the output matching network, the input matching network should be designed to provide a conjugate of the input impedance of the transistor while loaded by output matching. There is no general analytical equation to compute the input impedance. Therefore, this impedance is extracted by performing measurement based source-pull test. Depending on the results of this test a proper input matching structure from Fig. 2 or other configuration can be selected. The design space for source reflection coefficient can vary based on the type of the transistor and its power capability. The design process of input matching circuit for Cree GaN 25 W device based on source-pull measurement data is described in section IV (B).

IV. BROADBAND GaN CLASS-E PA DESIGN

In recent years GaN transistors have been often used in RF power amplifier designs due to their high power capability and improved power efficiency. In addition, their fairly high transition frequency makes them suitable for switching mode power amplifier designs where output harmonic frequencies impedances should be controlled as well as the fundamental frequency impedance. In this paper, a packaged GaN HEMT from Cree (CGH40025) has been used to design a broadband class-E power amplifier for 1.8 GHz–2.7 GHz LTE frequency range. Although there is a commercial nonlinear Advanced Design System (ADS) model is available for this device, load/source –pull measurement has been performed for different frequencies to obtain accurate optimum load and source impedances of this device. The packaged GaN Cree device has been mounted in Focus microwave passive load/source –pull measurement set-up test fixture and biased at $V_{GG} = -3.5$ and $V_{DD} = 30$ V. After calibrating the set-up optimum load impedances for maximum PAE and optimum source impedances for maximum gain as well as efficiency, and output power contours have been obtained for 2.14 GHz 2.45 GHz and 2.5 GHz.

These frequencies are selected because harmonic load terminations are only available for these frequencies. Fig. 7 shows the obtained optimum load and source reflection coefficients on the Smith chart for the entire frequency band (1.8 GHz - 2.7 GHz). The points are extracted by extrapolating the three-measured point in ADS schematic S-parameter simulation. The ideal optimum class-E load impedance is close to what is obtained from load-pull measurement according to Fig. 7. To design the broadband class-E PA input and output matching circuits should be designed so that they provide presented impedances in Fig. 7 pointed out two important points.

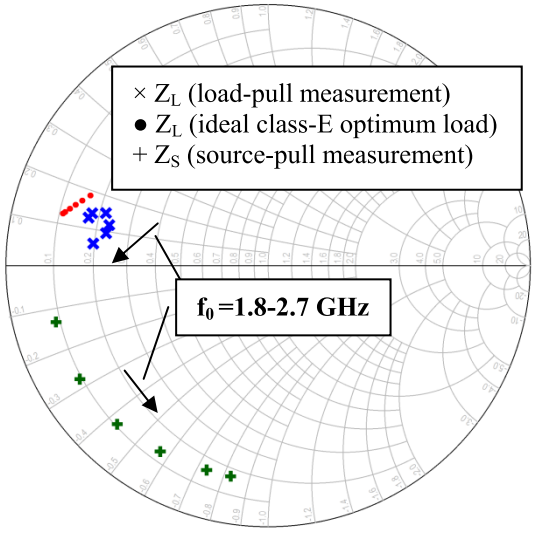

FIGURE 7. Optimum load impedances for maximum PAE and optimum source impedances for maximum gain obtained from load/source –pull measurement of CGH40025.

- Load reflection coefficients (Γ_L) in the targeted frequency range are gathered in a compact area of the Smith chart while source reflection coefficients expanded in a relatively wider area. This shows that two different topologies may be needed to realize these two groups of impedances.
- The optimum source and load impedances are spread counterclockwise as a function of frequency in the Smith chart, while a typical matching network response as a function of frequency is clockwise.

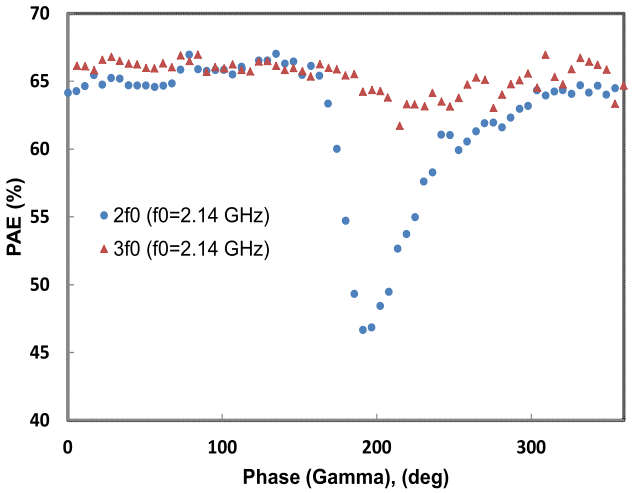

FIGURE 8. Power added efficiency versus phase variation of Γ_L at the second and third harmonic frequencies obtained from load-pull measurement at 2.14 GHz.

According to the class-E principle of operation, the device should be terminated to open circuit (high impedance) condition at the second and third harmonic frequencies. However, in practice, it is very challenging to terminate these harmonic with open circuit condition. For practical implementation, the load-pull measurement data shows that there is more freedom to select these harmonic impedances. For instance, Fig. 8 presents measured PAE results at 2.14 GHz by changing the phase of 2nd and 3rd harmonic load reflection coefficients while fundamental frequency load and source reflection coefficients are set to their optimum values shown in Fig. 7. Due to the available passive load-pull set-up limitations, the magnitude of the reflection coefficient at the 2nd and 3rd harmonic frequencies are set to 0.9 and 0.85 by a harmonic tuner.

Test results, depicted in Fig. 8, shows that if the magnitude of the load reflection coefficient at the 2nd harmonic frequency is close to unity its phase doesn't have a big influence on PAE, as long as it stays between 0° and 170°. For the 3rd harmonic load reflection coefficient, PAE remains almost unchanged for all the points near to the border of the Smith chart independent of its phase.

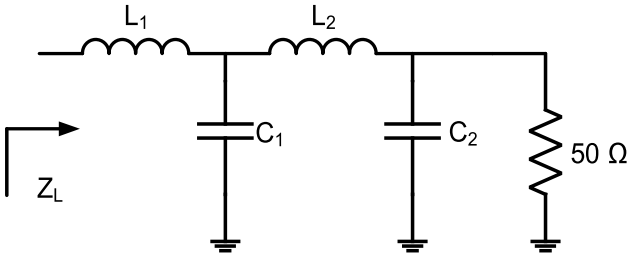

FIGURE 9. Broadband output matching circuit structure for class-E PA design.

A. BROADBAND OUTPUT MATCHING CIRCUIT DESIGN

To provide proper optimum load impedance for Cree 25W packaged device the matching circuit should be designed to transfer 50 Ω to the impedances shown in Fig. 7 (× symbol). As discussed in III (A) an appropriate lumped element circuit to reach this goal is configuration c shown in Fig.2 which is a low-pass impedance transformer network. However, in order to cover the targeted frequency band (1.8 GHz - 2.7 GHz) a ladder, the multi-stage low-pass network should be employed. The output matching circuit design in this paper is based on the Chebyshev low-pass impedance transformation network as presented in [18]. To start the design process a load impedance point obtained from load-pull measurement at 2.14 GHz is selected (Z_L = 12.7 + j*5.8Ω). This is the closest point to the center frequency (2.25 GHz) of the targeted frequency band for which the harmonic load-pull measurement couldn't be run due to the frequency limitation of the load harmonic tuner. Values of a four-element low-pass transformation network to convert 50 Ω to 12.5 Ω with a fractional bandwidth of 0.4 and in-band attenuation ripple of less than 0.015 dB are obtained using [13]. The synthesized two-stage low-pass impedance transformer structure is shown in Fig. 9. The calculated values from [13] assure that the reference impedance is transformed to 12.5 Ω, a close value to the real part of the selected complex load impedance for the design (Z_L = 12.7+j*5.8 Ω), in the targeted frequency band. These values are reported in Table 1 and used as a starting

TABLE 1. Output matching circuit components values.

Components	Values
L1	0.5 nH
C1	2.7 pF
L2	1.8 nH
C2	1.5 pF

point for optimization and synthesizing the required complex load impedance all over the frequency band.

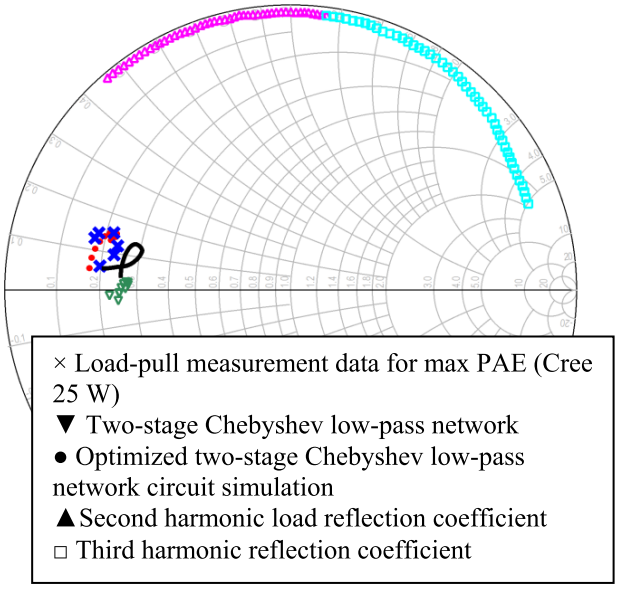

FIGURE 10. Load-pull measurement and simulation results of synthesized load reflection coefficient in different design steps for the targeted frequency band, (1.8 GHz - 2.7 GHz).

The reflection coefficient of the broadband output matching circuit with component values are presented in Table 1 is shown in Fig. 10 (▼ symbols). These component values are then optimized to provide the obtained optimum load reflection coefficient from load-pull measurements which are depicted in both Fig. 7 and Fig. 10 (× symbol). The components have been optimized using ADS schematic S-parameter and optimization simulations with goals defined for reflection coefficients at the start, stop and center frequencies of the band. Synthesized load reflection coefficient after optimizing the two-stage Chebyshev low-pass impedance transformer is shown in Fig. 10 (● symbols).

To implement the designed and optimized output matching circuit a few points should be considered.

- In every design and optimization steps, the components values have been tried to be kept as small as possible. Because, small capacitance has higher SRF and small inductance presents smaller resistance (greater Q), with lower SRF. In addition, inductors can be replaced by short narrow transmission lines which are preferred in broadband designs.
- Lumped element capacitors are preferred to capacitive open-ended stubs as long as their SRF is greater than the 3rd harmonic of the operating frequency. Low impedance open-ended transmission lines typically are frequency sensitive capacitances and would expand the load reflection coefficient response on the Smith chart and hence are not the best choice for broadband applications unless they are the only practical choice.
- Lumped element inductors though have typically much less SRF than lumped element capacitors and often present a significant series resistance which can degrade the efficiency. Thus, they are replaced by short narrow microstrip transmission lines in this paper.

By considering the above points, output matching layout has been EM co-simulated and optimized by using s-parameter model of the utilized American Technical Ceramic (ATC) capacitors. Fig. 10 shows the simulated load reflection coefficient (solid line). The 2nd and 3rd harmonic output reflection coefficients of this circuit are also shown in this figure (▲ and ■ symbols respectively). The maximum 2nd and 3rd harmonic load reflection coefficient phases are 130° and 82° which occur at 3.6 GHz and 5.4 GHz respectively. They lie in the acceptable design region given by Fig. 8.

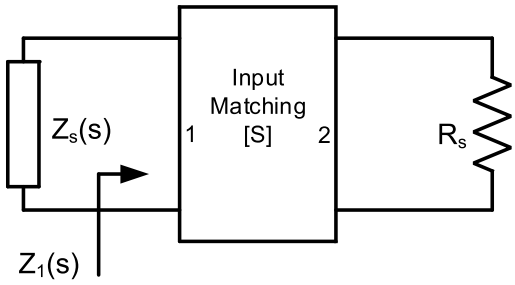

FIGURE 11. Block diagram of the input matching circuit terminated to source impedance and optimum input impedance at port 2 and 1 respectively.

B. BROADBAND INPUT MATCHING CIRCUIT DESIGN

The optimum input reflection coefficients for maximum gain over the broadband frequency range are dispersive over a greater area on the Smith chart as compared to the output reflection coefficient. The broadband matching theorem proposed in [19] suits better for realizing the optimum input reflection coefficient for maximum gain since it can theoretically map a real impedance to a set of frequency dependent complex impedance. Either the Chebyshev or Butterworth response can be selected for achieving the targeted gain response. The input matching circuit is shown in Fig. 11 and has been designed using the following sequential steps.

- A series RLC circuit is found to model the optimum input source impedance, shown in Fig. 7 (+ symbol), within the pass-band. Subsequently, load impedance function of the input matching circuit $Z_S(s)$ is determined.

- Non-sloped Chebyshev gain response of the matching network $G(-s^2)$, expressed in (4), is selected.

$$G(-s^2) = \frac{K_n}{1 + P_n^2(s')} \quad 0 \le K_n \le 1$$
$$P_n(s') = \varepsilon\, C_n(s')$$
$$s' = \frac{s^2 + \omega_0^2}{jBs} \quad B = \omega_2 - \omega_1\ \omega_0^2 = \omega_1\omega_2 \quad (4)$$

  where C_n is the n^{th} order Chebyshev polynomial of the first kind, ε is the ripple factor and ω_1 and ω_2 are the lower and upper pass-band frequencies.
- Using $G(-s^2)$ a minimum-phase bounded-real reflection coefficient p(s) has been found such that $p(s)p(-s) = 1 - G(-s^2)$
- Determined the positive-real restrictions, defined in [19] have been checked to make sure that the input impedance of the matching network $Z_1(s)$ will be positive–real. If the conditions are satisfied we go to the next step if not a different p(s) is chosen.
- The input impedance of the matching circuit has been obtained using the selected gain response G(s) and the determined minimum-phase real-bounded reflection coefficient p(s) and load impedance function $Z_s(s)$ as expressed in (5). The optimum input impedance $Z_s(s)$ is selected as a reference impedance for the input matching network shown in Fig. 11.

$$S_{11}(s) = \frac{Z_1(s) - Z_s(-s)}{Z_1(s) + Z_s(s)}$$
$$\Rightarrow Z_1(s) = \frac{2r_s(s)}{1 - S_{11}(s)} - Z_s(s) \quad (5)$$

  where $S_{11}(s)$ is a function of p(s).
- $Z_1(s)$ has been synthesized into a lumped element network by employing pole extraction method.

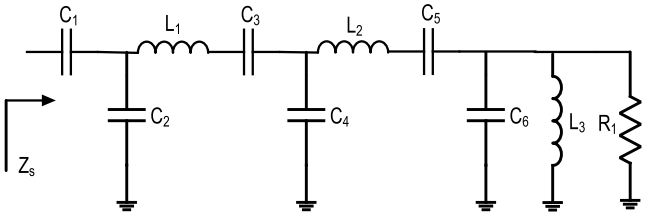

FIGURE 12. Ideal broadband input matching circuit.

The synthesized network is composed of reactive components and a non-50 Ω resistor as the load which should be transformed to the reference impedance (50 Ω). The designed ideal input matching circuit structure is presented in Fig. 12 and its corresponding components values are listed in Table 2. A fifth order circuit (n = 5) has been chosen to cover the targeted optimum input reflection coefficient points within the pass-band. The input reflection coefficient of this circuit is shown in Fig. 13 (• symbol). A broadband circuit with the greater order may present an input reflection coefficient closer to the targeted area shown in Fig. 13 (+ symbol)

TABLE 2. Ideal input matching circuit components values.

Components	Values	components	values
C1	7.2 pF	C6	1 pF
C2	5.4 pF	L1	3.5 nH
C3	15 pF	L2	22.5 nH
C4	2.1 pF	L3	6.5 nH
C5	0.26 pF	R1	91 Ω

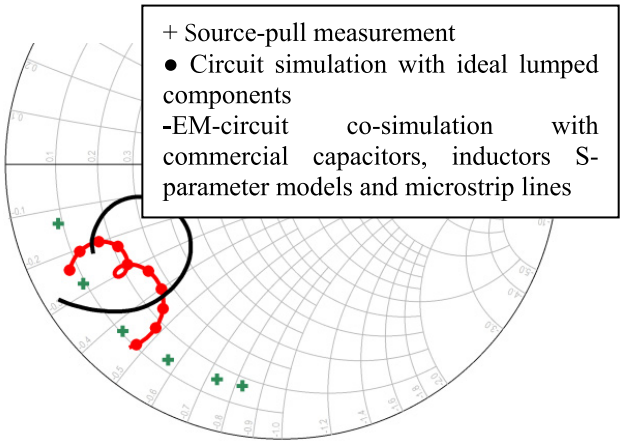

FIGURE 13. Input reflection coefficient simulation results of the designed input matching circuit and optimum input reflection coefficient for maximum gain obtained from source-pull measurement for 1.8 GHz - 2.7 GHz frequency band.

but at a price of greater complexity. A circuit with excessive complexity makes the post-fabrication tuning very complex and difficult. Therefore the order of the input matching circuit is constrained to 5 elements.

This ideal lumped-element broadband circuit then has been converted to a more realistic circuit by adding the components soldering pads and replacing the smaller inductances and a portion of the bigger ones by a short high impedance microstrip transmission line. The ideal capacitors and inductors are also replaced by S-parameter models of the available commercial components from American Technical Ceramics Corp. (ATC) and Coilcraft respectively. In input matching circuit design the restrictions on SRF and Q factor of the lumped elements are more relaxed since the response of the circuit is more critical at fundamental frequency f_0 and the losses presented by commercial inductors are not as critical as they are at the output matching circuit. The layout of the input matching circuit has been prepared in ADS and an EM-circuit co-simulation has been run to more accurately estimate the response of the circuit after fabrication. The result of this co-simulation is presented in Fig. 13 by a solid black line. The discrepancy between the realistic and ideal input matching circuit responses is due to adding the microstrip lines to connect the components, soldering pads, parasitics of the lumped components and the tolerance of the lumped components. Furthermore, the component values for the realistic circuit have been selected from the limited values of available commercial components and are not exactly what is obtained

from ideal optimization. However, an optimization using the commercial components models has been performed to find the optimum response by considering all the described non-idealities and limitations.

V. BROADBAND CLASS-E FABRICATION AND MEASUREMENT RESULTS

The designed and simulated input and output matching circuits described in Section IV have been fabricated on a Rogers' substrate (RO5870) with the Aluminum base. This substrate has $\varepsilon_r = 2.33$ and height (H) $= 20$ mils. Before building the power amplifier the two matching circuits are built and their input reflection coefficients are measured after soldering the components. Due to the tolerance of the commercial components and fabrication errors, the components have been altered to minimize the discrepancy between the measured and simulated reflection coefficient responses. Fig. 14 presents the simulated and measured input reflection coefficients of the input and output matching circuits when they are terminated with a 50 Ω load.

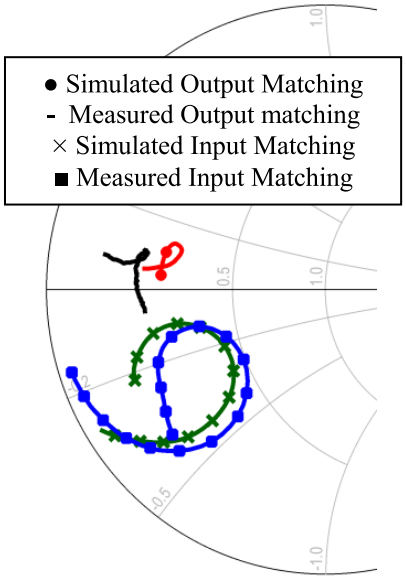

FIGURE 14. Measured and simulated input reflection coefficients of the designed and fabricated broadband input and output matching circuits for 1.8 GHz - 2.7 GHz frequency band.

Input and output matching integrated on a RO5870 substrate to make the broadband class-E power amplifier. A stabilizing circuit composed of a resistor and a capacitor in parallel has been designed and added at the gate of the transistor. The gate and drain of the device are biased through a 27 nH and a high current 22 nH inductors from Coilcraft respectively. The gate and drain bias voltages are set to −3.5 V and 30 V as they were during the load/source –pull measurements. The PA is driven by a 33 dBm continuous wave (CW) signal to ensure the transistor switch-like operation by using a wideband linear driver to amplify the signal generator output signal. The CW frequency sweep measurement results of the broadband class-E PA is shown in Fig. 15. The output power is measured using a Spectrum analyzer.

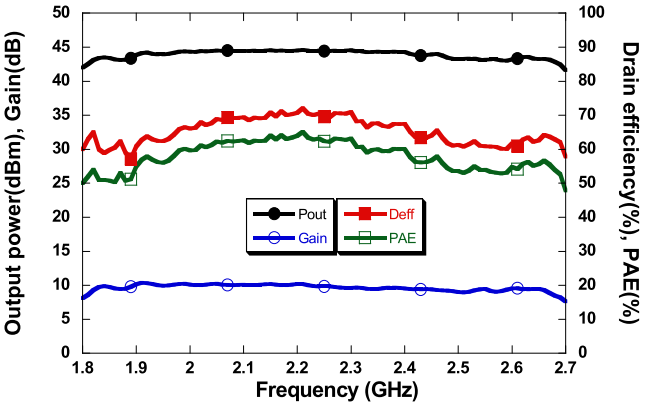

FIGURE 15. Measured results of frequency sweep test of the fabricated broadband class-E PA, the input power was set to 33 dBm.

The performance of the fabricated broadband PA under CW test as presented in Fig. 15 can be summarized as follows.

- The PA power added efficiency is greater than 48 % in 1.8 GHz - 2.7 GHz band with a peak of 65.2 % at 2.21 GHz.
- The PA's output power in this frequency range lies in the range of 16 W-29 W.
- The gain is greater than 8 dB all over the frequency range.
- In contrary to [11] the drain and gate bias voltages are kept constant in this test which provides a more practical test condition.

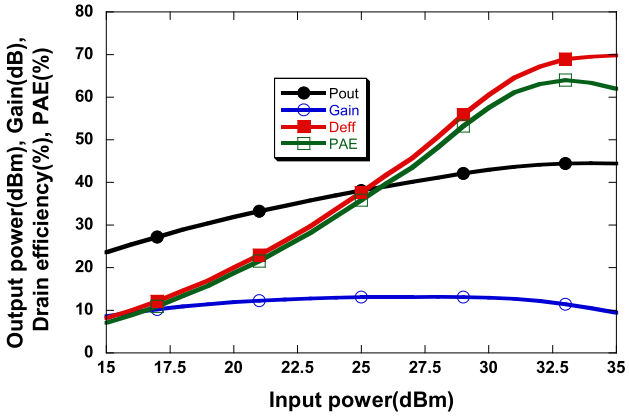

FIGURE 16. Measured results of input power sweep test of the fabricated broadband class-E PA at 2.14 GHz.

Power and drain voltage bias sweep test at 2.14 GHz has also been performed and their results are depicted in Fig. 16 and Fig. 17 respectively. The PA shows more than 50% PAE in 4 dB back off input power. Its drain efficiency remains almost constant when the drain bias voltage varies in the range of 10V-30V while its output power responds linearly to this variation. Although class-E PAs are not generally appropriate for conventional transmitters, the high back

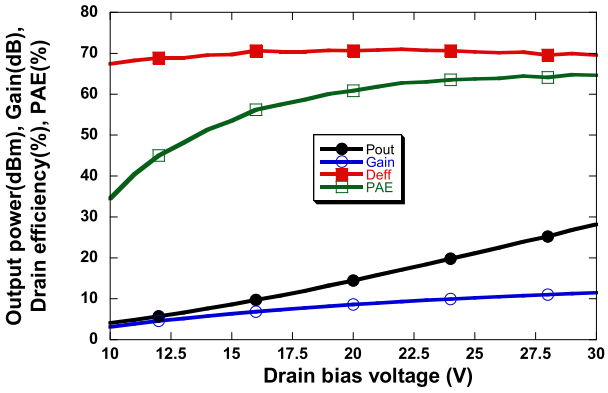

FIGURE 17. Measurement results of drain bias voltage sweep test of the fabricated broadband class-E PA at 2.14 GHz and for Pin = 33 dBm.

off power efficiency and relatively flat gain response of the fabricated PA shown in Fig. 16 which suggest that it can be used in conventional transmitters utilizing signals with small PAPR. Furthermore, it's fairly constant power efficiency and linear output power responses to the drain bias voltage variation illustrated in Fig. 17 show a good potential for being used in polar transmitters.

To evaluate the performance of the PA for a practical transmitter two tests under modulated signals have been performed. In the first test, the PA performance as a block in a conventional transmitter is tested. Since class-E PA should be driven by a constant envelop signal and in saturation, GSM signal which is a constant envelop signal is chosen for this test. Baseband I and Q files of a 0.27 KHz GSM signal are generated in ADS and are then loaded into an E4438C ESG vector signal generator using MATLAB. Fig. 18 shows the normalized power spectrum of this signal at the output of the ESG and PA. The signal is centered at 1.96 GHz.

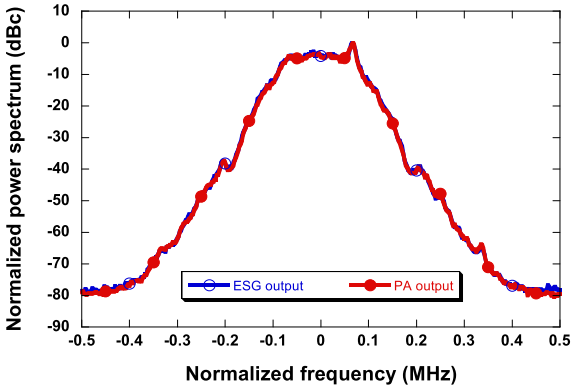

FIGURE 18. Output power spectrum of the broadband class-E PA and ESG vector signal generator driven by a 0.27 MHz GSM signal at 1.96 GHz carrier frequency.

The PA output signal quality is the same as the input signal while the measured output power and drain efficiencies are 43.8 dBm and 60 % respectively. These results prove that the designed PA amplifies the RF modulated GSM signal efficiently and with no reduction of the signal quality.

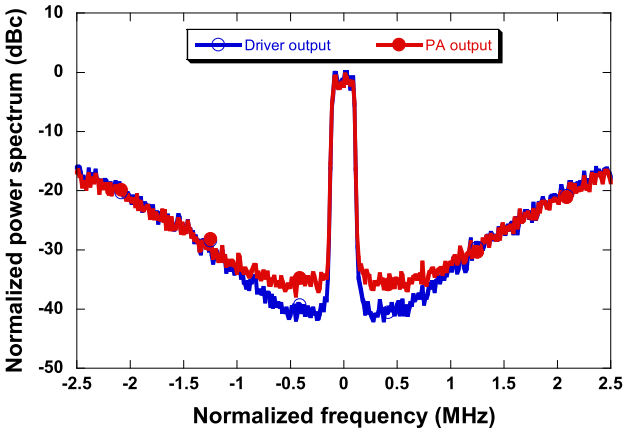

FIGURE 19. Output power spectrum of the linear driver and the broadband fabricated class-E PA driven by a delta-sigma modulated LTE downlink signal at 2.14 GHz carrier frequency.

The second test has been performed by sending a delta-sigma modulated LTE downlink signal to the PA. A 1.4 MHz LTE downlink signal which is an envelope varying signal with 10 dB PAPR has been generated in ADS. The Baseband I and Q files of this signal are then modulated by a second-order delta-sigma modulator in an ADS schematic simulation to provide a constant envelop signal. The PA is tested by this signal, loaded into E4438C ESG using MATLAB, at different frequencies. Fig. 19 shows the normalized output power spectrum of the driver and fabricated class-E PA driven by this signal at an instance frequency of 2.14 GHz. Two points are worth mentioning about this figure.

- The signal quality of the PA output declines by a small amount because the input signal is not a perfect pulse sequence due to measurements limitations.
- Although the LTE downlink signal generated by ADS has 1.4 MHz bandwidth, the actual signal sent to the PA has the smaller bandwidth. This is because of the limited sampling frequency of the available ESG.

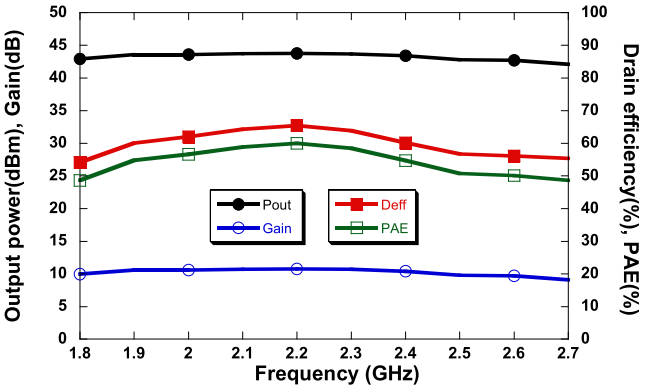

FIGURE 20. Measurement results of the broadband class-E driven by delta-sigma modulated LTE downlink signal.

The measured PA performance in the whole designed frequency band (1.8 GHz - 2.7 GHz) under the described LTE downlink signal drive is shown in Fig. 20. The output power

and gain are constant while PAE stays greater than 48 % over broadband. The adjacent channel power ratio (ACPR) is lower than −36 dBc for all frequency points in this test. The fabricated class-E PA shows linear and high-efficiency performance when is employed in a delta-sigma modulation based transmitter as proved by the delta-sigma modulated LTE downlink signal test.

VI. CONCLUSION

This paper presents a load/source –pull measurement-based approach to design a broadband class-E power amplifier at RF frequency for packaged transistors. The methodology is independent of the device technology and frequency as long as the available commercial lumped components can be used in the frequency of operation. 4 GHz is a rough estimation of the upper-frequency range of this method since most of the commercial inductors and capacitors are not very accurate beyond this frequency. It is shown in this paper that a low-pass multi-stage broadband impedance transformer with a small optimization process can always be used as an appropriate configuration for output matching circuit of a class-E PA while input matching configuration could be different according to the required device optimum input reflection coefficient for maximum gain. Broadband input and output matching circuits are designed for obtaining optimum input and output reflection coefficients from load/source–pull measurements. The broadband (40 % fractional bandwidth) 25 W GaN HEMT class-E PA is then prototyped in hybrid technology and its performance has been evaluated through different CW and modulated signal tests. Designed for LTE frequency range (1.8 GHz - 2.7 GHz), It has been shown that the fabricated PA operates properly when driven by LTE signal in delta-sigma modulation based transmitters.

REFERENCES

[1] S. C. Cripps, *Advanced Techniques in RF Power Amplifiers Design*. Norwood, MA: Artech House, 2002.
[2] T. Sharma, R. Darraji, F. Ghannouchi, and N. Dawar, "Generalized continuous class-F harmonic tuned power amplifiers," *IEEE Microw. Compon. Lett.*, vol. 26, no. 3, pp. 213–215, Mar. 2016.
[3] T. Sharma, R. Darraji, and F. Ghannouchi, "Design methodology of high-efficiency contiguous mode harmonically tuned power amplifiers," in *Proc. IEEE Radio Wireless Symp. (RWS)*, Austin, TX, USA, Jan. 2016, pp. 148–150.
[4] F. H. Raab, "Class-E, Class-C, and Class-F power amplifiers based upon a finite number of harmonics," *IEEE Trans. Microw. Theory Tech.*, vol. 49, no. 8, pp. 1462–1468, Aug. 2001.
[5] P. Aflaki and M. Helaoui, "Effect of the class of switching-mode power amplifiers on the efficiency of band-pass delta-sigma architectures," in *Proc. IEEE Eur. Microw. Integr. Circuits Conf. (EuMIC)*, Manchester, U.K., Oct. 2011, pp. 312–315.
[6] R. Negra and W. Bachtold, "Lumped-element load-network design for class-E power amplifiers," *IEEE Trans. Microw. Theory Techn.*, vol. 54, no. 6, pp. 2684–2690, Jun. 2006.
[7] T. Sharma, R. Darraji, P. Mousavi, and, F. M. Ghannouchi, "Generalized design of continuous-mode second harmonic tuned amplifiers," *Microw. Opt. Technol. Lett.*, vol. 58, no. 12, pp. 2787–2789, Sep. 2016.
[8] F. J. Ortega-Gonzalez, "Load–pull wideband class-E amplifier," *IEEE Microw. Wireless Compon. Lett.*, vol. 17, no. 3, pp. 235–237, Mar. 2007.
[9] T. Sharma, R. Darraji, and F. Ghannouchi, "A methodology for implementation of high-efficiency broadband power amplifiers with second-harmonic manipulation," *IEEE Trans. Circuits Syst. II, Exp. Briefs*, vol. 63, no. 1, pp. 54–58, Jan. 2016.
[10] A. A. Tanany, A. Sayed, and G. Boeck, "Broadband GaN switch mode class E power amplifier for UHF applications," in *IEEE MTT-S Int. Microw. Symp. Dig.*, Jun. 2009, pp. 761–764.
[11] C.-H. Lin and H.-Y. Chang, "A high efficiency broadband class-E power amplifier using a reactance compensation technique," *IEEE Microw. Wireless Compon. Lett.*, vol. 20, no. 9, pp. 507–509, Sep. 2010.
[12] K. Chen and D. Peroulis, "Design of highly efficient broadband class-E power amplifier using synthesized low-pass matching networks," *IEEE Trans. Microw. Theory Techn.*, vol. 59, no. 12, pp. 3162–3173, Dec. 2011.
[13] N. O. Sokal and A. D. Sokal, "Class E-A new class of high-efficiency tuned single-ended switching power amplifiers," *IEEE J. Solid-State Circuits*, vol. SSC-10, no. 3, pp. 168–176, Mar. 1975.
[14] P. Aflaki, R. Negra, and F. M. Ghannouchi, "Enhanced architecture for microwave current-mode class-D amplifiers applied to the design of an S-band GaN-based power amplifier," *IET Microw., Antennas Propag.*, vol. 3, no. 6, pp. 997–1006, Sep. 2009.
[15] T. Sharma *et al.*, "High-efficiency input and output harmonically engineered power amplifiers," *IEEE Trans. Microw. Theory Techn.*, to be published, doi: 10.1109/TMTT.2017.2756046.
[16] M. M. Ebrahimi, M. Helaoui, and F. M. Ghannouchi, "Improving Coding Efficiency by compromising linearity in delta-sigma based transmitters," in *Proc. IEEE Radio Wireless Symp. (RWS)*, Santa Clara, CA, USA, Jan. 2012, pp. 411–414.
[17] T. Sharma, R. S. Embar, D. Holmes, R. Darraji, J. Jones, and F. Ghannouchi, "Harmonically engineered and efficiency enhanced power amplifier design for P3dB/back-off applications," in *IEEE MTT-S Int. Microw. Symp. Dig.*, Honolulu, HI, USA, Jun. 2017, pp. 789–792, doi: 10.1109/MWSYM.2017.8058696.
[18] M. P. van der Heijden, M. Acar, and J. S. Vromans, "A compact 12-watt high-efficiency 2.1-2.7 GHz class-E GaN HEMT power amplifier for base stations," in *IEEE MTT-S Int. Microw. Symp. Dig.*, Jun. 2009, pp. 657–660.
[19] G. L. Matthaei, "Tables of Chebyshev impedance—Transforming networks of low-pass filter form," *Proc. IEEE*, vol. 52, no. 8, pp. 939–963, Aug. 1964.
[20] T. T. Ha, *Solid-State Microwave Amplifier Design*. New York, NY, USA: Wiley, 1981.

TUSHAR SHARMA (S'10) received the B.Tech. degree in electronics and communications engineering from Guru Gobind Singh Indraprastha University, Delhi, India. He is currently pursuing the Ph.D. degree with the University of Calgary, Calgary, AB, Canada. In 2016 and 2017, he joined NXP Semiconductors, Chandler, AZ, USA, as a Research and Development Design Intern. He was a recipient of the Izaak Walton Killam Pre-Doctoral Scholarship, the AITF Doctoral Scholarship, the Alberta Transformative Talent Scholarship, the Academic Excellence Award, and the Research Productivity Award. He has authored and co-authored over 16 refereed publications. His current research interests include high-efficiency broadband RF power amplifiers, waveform engineering techniques for power amplifiers, and active/passive load-pull techniques.

POUYA AFLAKI (S'06–M'12) received the M.Sc. degree in electrical engineering from the Amirkabir University of Technology (Tehran Polyphonic), Tehran, Iran, in 2006, and the Ph.D. degree in electrical engineering from the University of Calgary, Calgary, Canada, in 2011. He is currently a Power Amplifier Design Engineer in Syntronic Research and Development, Ottawa, Canada. His research interests include Doherty and switching-mode microwave power amplifiers, microwave passive circuits design, advanced transmitter architectures, linearization techniques and large-signal device modeling.

MOHAMED HELAOUI (S'06–M'09) received the M.Sc. degree in communications and information technology from the École Supérieure des Communications de Tunis, Tunisia, in 2003, and the Ph.D. degree in electrical engineering from the University of Calgary in 2008. He is currently an Assistant Professor with the Department of Electrical and Computer Engineering, University of Calgary. His research activities have led to over 60 publications and seven patents (pending). His current research interests include digital signal processing, power efficiency enhancement for wireless transmitters, switching mode power amplifiers, and advanced transceiver design for software defined radio and millimeter-wave applications. He is a member of the COMMTTAP Chapter in the IEEE Southern Alberta Section.

FADHEL M. GHANNOUCHI (S'84–M'88–SM'93–F'07) is currently a Professor, the Alberta Innovates/the Canada Research Chair, and the Founding Director of the iRadio Laboratory, Department of Electrical and Computer Engineering, University of Calgary, Calgary, AB, Canada. He held several invited positions at several academic and research institutions in Europe, North America, and Japan. He has provided consulting services to many microwave and wireless communications companies. He has authored or co-authored over 650 publications. He holds 16 U.S. patents with four pending. His current research interests include microwave instrumentation and measurements, nonlinear modeling of microwave devices and communications systems, design of power- and spectrum-efficient microwave amplification systems, and design of intelligent RF transceivers for wireless and satellite communications.